Rapid Bottom Melting Widespread near Antarctic Ice Sheet Grounding Lines

E. Rignot [1] and S. Jacobs [2]

As continental ice from Antarctica reaches the grounding line and begins to float, its underside melts into the ocean. Results obtained with satellite radar interferometry reveal that bottom melt rates experienced by large outlet glaciers near their grounding lines are far higher than generally assumed. The melting rate is positively correlated with thermal forcing, increasing by one meter per year for each 0.1^{o}C rise in ocean temperature. This renders glaciers and ice shelves where deep water has direct access to grounding lines vulnerable to ongoing increases in ocean temperature.

Submitted to *Science*

Manuscript Number xxx

[1]Jet Propulsion Laboratory, California Institute of Technology, Mail Stop 300-235, Pasadena, CA 91109-8099, USA; ph. 818/354-1640; fax. 818/393-3077; email: eric@adelie.jpl.nasa.gov

[2]Columbia University, Lamont-Doherty Earth Observatory; Route 9W, Palisades, NY 10964-8000, USA; ph. 914/365-8326; fax. 914/365-8157; email: sjacobs@ldeo.columbia.edu.

The undersides of ice streams flowing from the Antarctic continent typically melt into the ocean where they cross the grounding line and begin to float as ice shelves and ice tongues (*1*). Unlike melting under the grounded ice sheet, processes beneath floating glaciers are governed by the transport of ocean heat and by the dependence of the seawater freezing temperature on pressure (*2*). This allows sensible heat to be obtained both from the cold dense shelf waters resulting from sea ice formation, and from 'warm deep' water that intrudes onto the continental shelf and flows into ice shelf cavities. Bottom melting freshens and cools the seawater, adding buoyancy that drives upwelling as the ice shoals seaward. In some regions, the rising seawater-meltwater mixture may drop below the in situ freezing point to form 'marine' ice that can comprise a substantial part of ice shelf volume (*3*,*4*). Where the continental shelf is broad and the inflows are cold and dense, some of the meltwater-laden outflows eventually sink and contribute to the formation of bottom water, which ventilates the deepest parts of the World oceans (*5*). Net basal melting beneath the 1.6 x 10^6 km^2 floating portion of the Antarctic Ice Sheet (*6*), adjusted for recent lower estimates for the larger ice shelves (*4*,*7*), averages about 40 cm/year. But much of the actual melting occurs in the deepest parts of the sub-ice-shelf cavities where direct measurements are unavailable, and would be very difficult to acquire.

Here we calculate basal melt rates at 22 of these remote, interior regions, using satellite radar interferometry observations of grounding line position, ice velocity, and surface topography of outlet glaciers that nourish ice shelves or ice tongues (*8*). With this technique, grounding lines are precisely located, and are often found to lie tens of kilometers landward of previously estimated positions (*13*). Basal melting calculations assume mass conservation and steady-state conditions between the grounding line and a flux gate located about one glacier width downstream (*14*). Thickness changes due to short-term variability in ice velocity, snow accumulation and surface ablation are believed to be small compared to the large bottom melt rates obtained.

We focus on melt rates near the grounding lines of deep-draft outlet glaciers because continental ice discharge is principally controlled by the channelized flow of these ice streams into the ocean (Figure 1). If these regions are the locus of high basal melting, the potential exists for substantial ocean control over ice shelf, if not ice sheet, mass balance (*15 – 17*). Indirect observations and computer models have suggested high basal melting in the proximity of deep grounding lines, and show that melting efficiency will decrease as buoyant plumes lose heat and rise to shallower depths along ice-ocean interfaces (*18, 19*). It is therefore not the average ice shelf melt rate, but the melt rate near the grounding line that will have the greatest impact on ice flow dynamics. As the properties and circulation of the ocean are modified by climate change, a corresponding change in the rate of basal melting in this region may alter ice thickness and motion enough to influence ice shelf stability.

The basal melt rates for the 22 glaciers shown in Figure 1 are listed in Table 1. The spectrum of values ranges from ≤ 4 m/year for several glaciers that flow into the Filchner-Ronne Ice Shelves to > 40 m/year for Pine Island Glacier. The wide range is consistent with earlier studies of several of the individual glaciers, using a variety of methods (*20 – 25*), and stems from quite different grounding line drafts, seawater temperatures, and uncertainties in ice thickness. Nevertheless, most of the melt rates we calculate near glacier grounding lines exceed the area-average rates for the largest ice shelves by 1-2 orders of magnitude.

The Table 1 melt rates are strongly correlated with ocean thermal forcing (Fig. 2), with a correlation R2 ≥ 0.8 (Fig. 2). The lateral spread of values around a linear regression results from uncertainties in ocean temperature, ice thickness, and the steady-state assumption. The use of maximum draft for the calculation slightly overestimates thermal driving, increasing R2 by 0.05 and decreasing the regression slope by 10%. Melt rate also depends on how rapidly ocean heat can be delivered to the basal ice, in turn a function of the density field, tidal mixing, sea floor topography and cavity shape (*26, 27*). Those factors vary with location, and are not well known at the present time. For example, the adjacent

Mertz/Ninnis pair in Table 1 apparently have similar grounding line ice flux and ocean forcing, but divergent melt rates. Their floating glacier tongues appear to be at opposite ends of advance and decay cycles (*28*), and have grounding lines at different distances from the general trend of the coastline, which may be important (*21*). The weakly-melting Ninnis remnant has also been accompanied for more than a decade by large grounded icebergs that may reduce the strength of the local circulation (*29*).

The largest thermal forcing, nearly 4°C above the in situ melting point (Fig. 2), is associated with the Pine Island, Thwaites and Smith glaciers that flow into the Amundsen Sea. This results from the nearly unaltered circumpolar deep water that extends southward across the floor of the Antarctic continental shelf in Pine Island Bay (*6*). The poor fit for Smith Glacier could indicate a blocking sill between its grounding line and deep water in the Bay, consistent with the presence of numerous ice rises in radar interferometry observations of the ice shelf. Deep water influence wanes toward the west, but clearly impacts the Kohler and Land glaciers (Table 1). Water warmer than +1.0^{o}C also floods the deeper shelf regions in the Bellingshausen Sea, but its effects are strongest where grounding lines are deepest. Default ocean temperatures of -2°C were assumed beneath glaciers entering the large ice shelves, from measurements beneath the Ronne Ice Shelf (*7*). Ocean temperatures will be colder (smaller Δ T in Table 1) if the outflow from a deep grounding line is advected past a shallower grounding line downstream.

The $B/\Delta T$ of 10/1 (m/^{o}C) in Fig. 2 is similar to that obtained for icebergs in warmer ocean water (*30*). Such studies typically assume negligible melting in water near the freezing point on the Antarctic continental shelf. Where grounding lines are deep, however, melt rates can exceed 20 m/year in water at -2°C, close to the ambient temperature for most of our study areas. Thermal forcing is thus high for glaciers like Lambert and David, which have grounding lines that reach depths of 3 km below sea level (Table 1). As a result, David Glacier loses 68 percent of its mass from bottom melting within 20 km of the grounding

line, driving an upwelling of 'supercooled' water, and the possible deposition of enough marine ice to preserve a lengthy Drygalski Ice Tongue (*21*).

The Shirase Glacier in East Antarctica has a relatively shallow grounding line (Table 1) in a region generally characterized by cold shelf water. Its high thermal forcing results from April and August ocean temperatures of +0.15^{o}C at depths below 900 m, landward of a sill on the outer shelf (*31*). This indicates that relatively warm modified deep water has year-round access to the Shirase grounding line. Modified circumpolar deep water is known to upwell at other locations along the East Antarctic continental shelf, and will increase grounding line melt rates where its density allows it to intrude along the sea floor.

Our results demonstrate that bottom melting near an ice shelf grounding line is strongly leveraged by the temperature of the seawater that comes into contact with the ice in that region. A rise in ocean temperature that increases the bottom melt rate will steepen the ice thickness gradient at the grounding line. This will increase the driving stress and flow velocity, and it will reduce the ice-shelf resistance to inland flow of ice, potentially increasing ice discharge into the ocean. If enhanced melting caused a grounding line to move landward into a deeper basin, a positive feedback would occur as the ocean progressively reached deeper ice. Conversely, a decrease in the melt rate, or a grounding line moving upslope, would stabilize the glacier by thickening and lowering its velocity (*17*).

Although the dynamic coupling between grounded and floating ice is complex, ice flow models have been developed to predict the response of the Antarctic Ice Sheet to a change in climate (*32,33*). Such models show that ice sheet area and volume would decline at area-averaged ice shelf melt rates near and above 1 m/year. With the grounding line melt rates listed in Table 1, the existing ice sheet models would probably not be able to maintain the ice sheet in a state of mass balance. If warmer winters reduced sea ice production and the flow of dense shelf water beneath the ice, bottom melting could decrease if that inflow is not replaced by warm deep water (*34*). The projected melt reduction in that scenario is only

10 percent, however, for an air temperature rise of 3°C in a century. Air temperature has risen at that rate over recent decades at Scott Base in the southwest Ross Sea, accompanied by a decline in salinity (*35*). No change has been observed in the Ross Ice Shelf thickness during the 1990s (*36*).

The potential impact of basal melting on short-term (<century) ice sheet stability is greatest in regions where deep water has direct access to glacier grounding lines. Those areas now occur mainly in the SE Pacific - West Antarctic sector (*6*), but also include East Antarctica, as shown by the Shirase Glacier. It remains to be determined how much a stronger pycnocline beneath a fresher surface layer will increase the temperature of warm deep water (*37*), and whether less sea ice and dense shelf water production, or increased melting, will change the transport of that deep water onto the Antarctic continental shelf. Ocean temperatures directly seaward of Antarctica's continental shelf break have risen by 0.2°C over recent decades (*35,38*), sufficient to increase basal melting by 2 m/year where that change has reached vulnerable grounding lines. This may account for the rapid thinning of ice shelves in the western Amundsen Sea (*24,25,36,39*), which in turn may play an essential role in the observed acceleration of their nourishing glaciers (*40*).

References and Notes

1 G. de Q. Robin, *J. Glaciol.* **24**, 259 (1979).

2 C. S. M. Doake, *Polar Record* **18** 37 (1976).

3 Oerter, H. *et al.*, *Nature* **358**, 399 (1992).

4 Grosfeld, K. *et al.*, *Ant. Res. Ser.* **75**, 319 (American Geophysical Union, Washington D.C. 1998).

5 A. H. Orsi, S. S. Jacobs, A. L. Gordon, M. Visbeck, *Geophys. Res. Lett.* **28**(15), 2923 (2001).

6 S. S. Jacobs, H. H. Hellmer, A. Jenkins, *Geophys. Res. Lett.* **23**, 957 (1996).

7 K. W. Nicholls, K. Makinson, *Ant. Res. Ser.* **75**, 301 (American Geophysical Union, Washington D.C. 1998).

8 Grounding lines were mapped using a differential interferometry technique applied to ERS interferometry data collected in 1992, 1994 and 1996 with a positional accuracy of 50 m (*9*) (Table 1). Ice velocity was mapped in vector form with ERS interferometry data collected north of 79°S latitude with a precision of a few meters per year where crossing swaths were available, otherwise combining interferometry data with speckle tracking along the satellite track with a precision of a few tens of meters per year (*10*). Velocity control was provided by motionless areas. Tidal corrections were applied on observed ice-shelf velocities using predictions from the FES99 tidal model (*11*). For glaciers located south of 79°S latitude, we employed Radarsat radar data collected in 1997 to map the ice velocity using speckle tracking both along and across the satellite track directions, with a precision of a few meters per year. The grounding line position of the glaciers surveyed in 1997 with Radarsat was mapped from hydrostatic equilibrium of the ice, with a precision of 1 km, by comparing ice shelf elevations with BEDMAP thicknesses (*12*). Grounding-line ice thickness for all glaciers was inferred from hydrostatic equilibrium constrained by existing thickness measurements where available, and assuming a default sea-water and ice density profile elsewhere.

9 E. Rignot, S. Gogineni, W. Krabill, S. Ekholm, *Science* 276, 934 (1997)

10 R. Michel and E. Rignot, *J. Glaciol.* **45**(149), 93 (1999).

11 F. Lefevre, F. H. Lyard, C. Le Provost, *Geophys. Res. Lett.* **27** (17), 2717 (2000).

12 M. B. Lythe, D. G. Vaughan, *J. Geophys. Res.* **106**(B6), 11,335 (2001).

13 British Antarctic Survey's Antarctic Digital Data base,

http://www.nbs.ac.uk/public/magic/add_download.html

14 Conservation of ice mass between the grounding line (GL) and a flux gate located downstream (DG), bordered by distinct flow bands, dictates that ice-shelf thickening over the ice-shelf area, *ISA*, in between the two gates, $\partial H/\partial t$ (positive for thickening), equals the sum of surface accumulation, A, minus the basal accumulation, B (positive for melting), and the difference in ice flux between the two gates per unit area,

$$\partial H/\partial t = A - B + (\phi_{GL} - \phi_{DG})/ISA \quad (1)$$

Under steady state conditions, $\partial H/\partial t = 0$, and neglecting surface melt and accumulation (< 0.5 m/year) compared to basal melting, B is equal to the decrease in ice flux per unit area. If the ice shelf is thickening (thinning) and ice flow is steady, then B would be lower (higher) than calculated under steady-state conditions.

15 J. Weertman, *J. Glaciol.* **13**(67), 3 (1974).

16 C. J. Van der Veen, *Ann. Geophys., Ser. B* **4**(1), 45 (1986).

17 R. H. Thomas, *J. Glaciol.* **24**(90), 167 (1989).

18 H. H. Hellmer, S. S. Jacobs, A. Jenkins. in *Antarct. Res. Ser.* 75, 83-99 (1998).

19 A. Jenkins, in *Ice in the Climate System* Ed. by W.R. Peltier, pp. 217-235, (Springer-Verlag, Berlin 1993).

20 A. Lambrecht, C. Mayer, H. Oerter, U. Nixdorf. *Ann. Glaciol.* **29**, 250 (1999).

21 M. Frezzotti, I. E. Tabacco, A. Zirizzotti, *Ann. Glaciol.* **46**(153), 253 (2000).

22 A. M. Smith, *J. Geophys. Res.* **101**(C10) 22,749 (1996).

23 J. R. Potter, J. G. Paren, *Antarct. Res. Ser.* **43**, 35 (1985).

24 E. Rignot, *Science* **281**, 549 (1998).

25 E. Rignot, *J. Glaciol.* **47**(157), 213 (2001).

26 D. R. MacAyeal, *J. Geophys. Res.* **89**(NC1) 597 (1984).

27 H. H. Hellmer, S.S. Jacobs, *J. Geophys. Res.* **97**(C12) 20,305 (1992).

28 G. Wendler, K. Ahlnas, C. S. Lingle, *J. Glaciol.* **42**(142), 447 (1996).

29 O. A. Nøst, S. Østerhus, *Ant. Res. Ser.* **75**, 267 (American Geophysical Union, Washington D.C. 1998).

30 W. F. Budd, T. H. Jacka, V.I. Morgan, *Ann. Glaciol.* **1**, 103 (1980).

31 S. Ushio, T. Takizawa, "Oceanographic data in Lutzow-Holm Bay of Antarctic Climate Research Programme from March 1990 to January 1991" (Japanese Antarctic Research Expedition Data Reports, 184, Nat'l Inst. of Polar Res., Tokyo, 1993).

32 P. Huybrechts, J. de Wolde, *J. Climate* **12**(8), 2169 (1999).

33 R. C. Warner, W. F. Budd, *Ann. Glaciol.* **27**, 161 (1998).

34 K. Nicholls, *Nature* **388**(6641), 460 (1997).

35 S. S. Jacobs, C. F. Giuvili, subm. to *Science.*

36 J. Zwally, A. C. Brenner, H. Cornejo, *J. Glaciol.*, in press.

37 A. Gordon, "Comments about the ocean role in the Antarctic glacial ice balance" (Proc. CO_2 Res. Conf. Science and Consensus, 19-23 Sep 1982, Berkeley Springs, IV.76-IV.86, 1983).

38 R. Robertson, M. Visbek, A. L. Gordon, E. Fahrbach, *Deep-Sea Res.*, in press.

39 A. Shepherd, D. Wingham, J. A. D. Mansley, *Geophys. Res. Lett.*, submitted.

40 E. Rignot, D. G. Vaughan, M. Schmeltz, T. Dupont, D. MacAyeal, *Ann. Glaciol.* **34**, in press.

41 UNESCO "Freezing point of seawater" (Eighth report of the Joint Panel of Oceanographic Tables and Standards) (UNESCO Technical Papers in Marine Science 28, 29-35, 1978).

42 We thank the European Space Agency, the Canadian Space Agency, and the Alaska SAR Facility for providing the ERS and Radarsat satellite data used in this project. Funding for this project was provided by a research contract with the National Aeronautics and Space Administration's Cryospheric Sciences Program, and by the National Science Foundation, Office of Polar Programs.

Table 1. Basal melt rates of Antarctic glaciers directly seaward of their grounding lines, assuming steady-state conditions. Yr, year ice velocity was measured (92, 94 and 96 is ERS, 97 is Radarsat); $Hp(Hm)$, peak (mean) ice thickness at grounding line; ϕ_{GL}, grounding line ice flux; ISA, ice shelf area between GL and DG gates; ϕ_{DG}, ice flux at the downstream gate; B, calculaled basal melt rate; ΔT, temperature differential between the estimated in situ sea-water temperature and the melting point of ice at a draft calculated as 0.88 Hp. Meters/year and km^3/year are in ice equivalent.

Glacier/Ice Shelf	Yr	$Hp(Hm)$ (km)	ϕ_{GL} (km^3/year)	ISA (km^2)	ϕ_{DG} (km^3/year)	B (m/year)	ΔT (^{o}C)
Pine Island (PIG)	96	1.3(1.0)	75.1±4	795	40.1±2	44±6	3.9
Thwaites (TWH)	96	1.0(0.9)	36.0±3	413	21.8±2	34±9	3.6
Smith/Crosson (SMI)	96	1.2(1.0)	19.3±2	341	13.1±1	18±8	3.7
Kohler/Dotson (KOH)	96	1.2(1.1)	9.9±1	210	5.8±0.5	20±5	2.8
Land (LAN)	96	1.0(0.9)	11.1±1	167	8.9±1	13±6	1.6
Byrd/Ross (BYR)	97	1.9(1.8)	23.6±2	533	15.0±1	16±4	1.3
David/Drygalski (DAV)	96	3.2(1.9)	15.6±2	362	5.0±0.5	29±5	2.1
Ninnis (NIN)	96	1.7(1.2)	21.9±3	406	19.9±2	5±7	1.1
Mertz (MER)	96	1.3(1.1)	19.1±2	375	12.9±1	17±6	0.9
Totten (TOT)	96	2.5(1.7)	69.6±7	1030	42.9±4	26±8	1.7
Denman/Shackleton(DEN)	96	1.9(1.8)	31.9±4	616	15.3±2	27±7	1.3
Scott/Shackleton(SCO)	96	1.7(1.3)	9.2±2	482	2.3±0.5	14±4	1.1
Lambert/Amery (LAM)	96	3.0(2.3)	57.5±5	952	28.4±2	31±5	1.9
Shirase (SHI)	96	1.2(0.9)	15.1±2	214	10.6±1	21±10	2.9
Jutulstraumen/Fimbul(JUT)	94	1.3(1.2)	13.4±1	391	11.9±1	4±3	0.9
Stancomb-Wills (STA)	96	1.2(0.9)	16.6±2	465	14.8±1	4±4	0.8
Slessor/Filchner(SLE)	97	1.6(1.4)	29.0±2	2806	25.0±2	1±1	1.0
Recovery/Filchner(REC)	97	1.7(1.3)	26.1±3	715	24.0±2	3±5	1.0
Institute/Ronne (INS)	97	1.2(1.1)	24.9±2	1078	24.8±2	0±3	0.7
Rutford/Ronne (RUT)	92	2.2(1.7)	17.6±2	785	8.7±1	11±3	1.4
Carlson/Ronne (CAR)	92	1.4(1.4)	2.6±0.2	362	1.0±0.1	5±1	0.8
Evans/Ronne (EVA)	96	2.2(1.5)	50.6±5	2205	18.9±2	14±2	1.4

FIGURE CAPTIONS

Fig. 1. Location map of the 22 Antarctic glaciers and ice tongues listed in Table 1. The ADD coastline (*13*) (ice front position and grounding line) is black, the drainage basins are outlined in green, the InSAR-derived grounding-line flux gates are red and ice shelves are blue. The 22 glaciers together drain more than 1/3 of the area of continental Antarctica, funneling the ice via a network of ice streams through narrow exit gates. The flux gates of THW, SMI, LAN, STA and REC only encompass the central, faster-moving, thicker part of those glaciers.

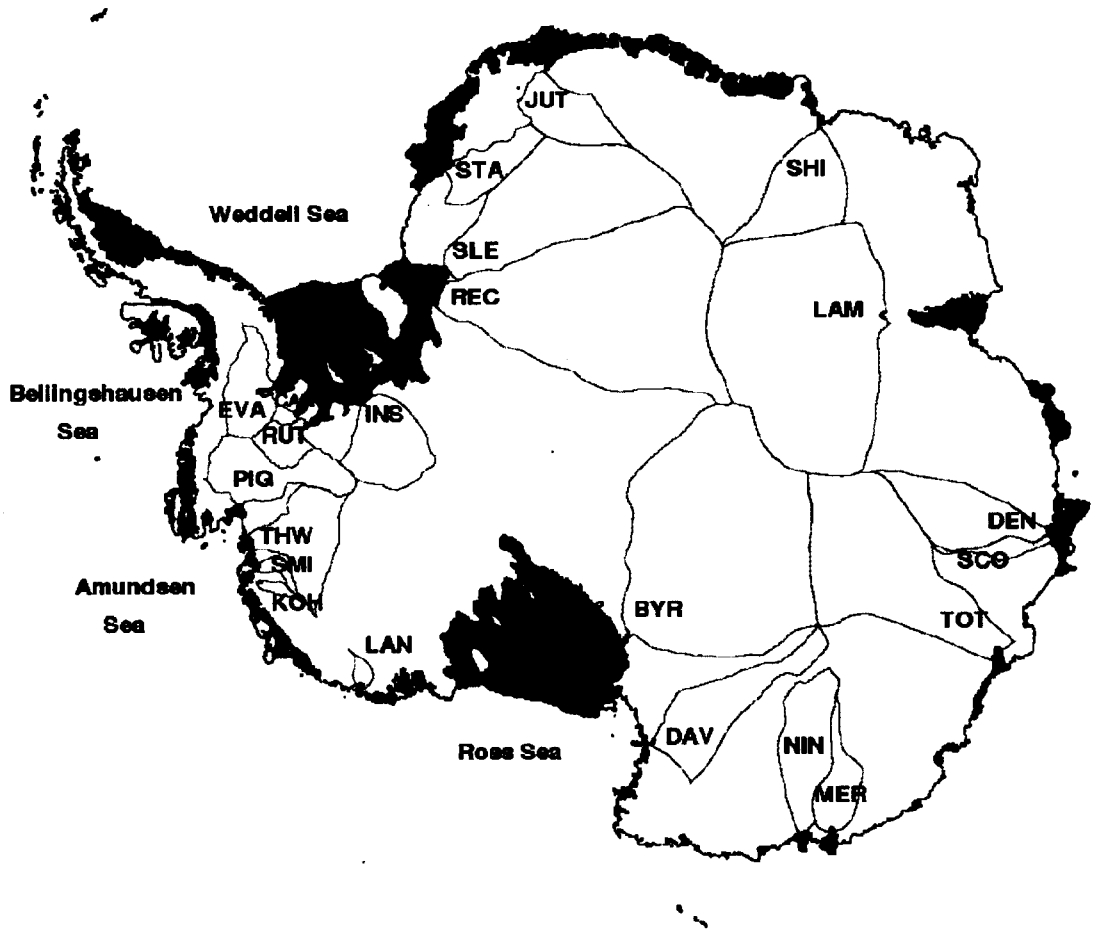
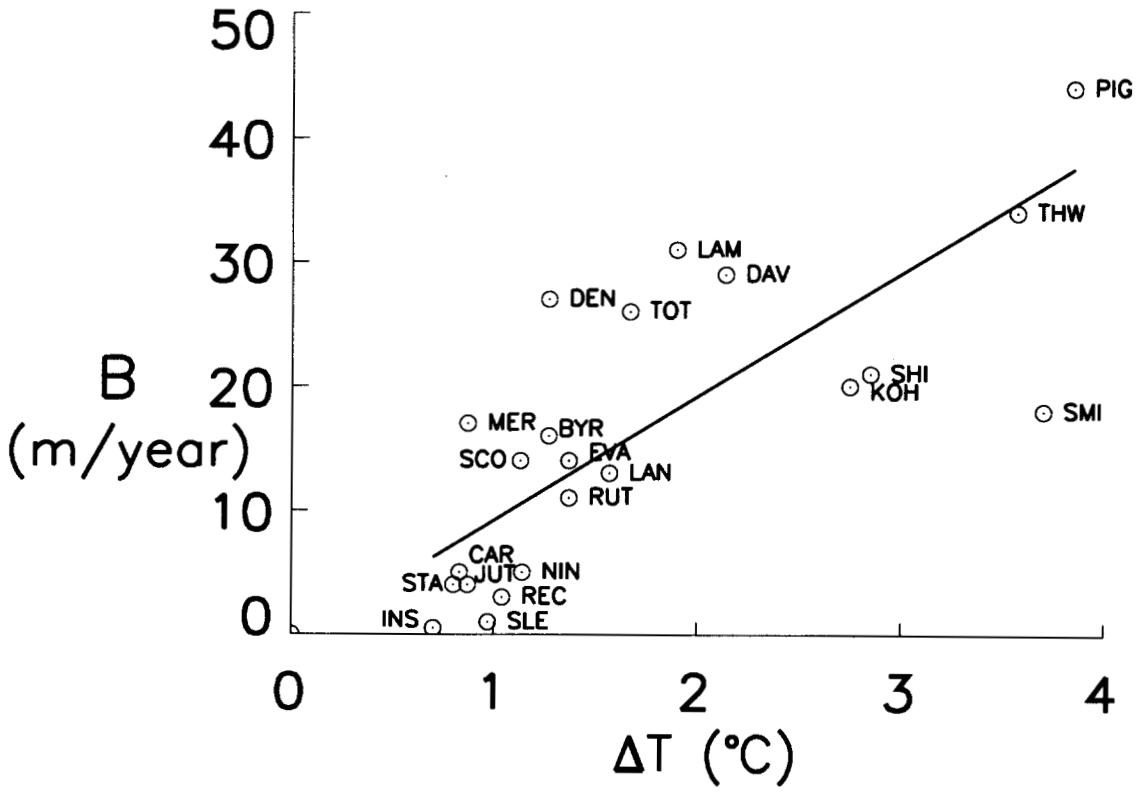
Fig. 2. Basal melt rates directly seaward of the grounding lines of Antarctic glaciers, vs thermal forcing by the ocean. The melt rate, B, is calculated from satellite radar interferometry observations of ice velocity and applies to the *ISA* (Table 1) between the grounding line and a flux gate located about one glacier width downstream. Thermal forcing, ΔT, is the difference between the nearest in situ ocean temperature measurement and the seawater freezing point (*41*) at a depth of 0.88 Hp (Table 1, (*25*)). The regression, $B = 9.95\ \Delta T - 0.75$, R2 = 0.9, without Smith Glacier (SMI) but with a single control at (0, 0), indicates that a 1°C increase in effective ocean temperature will increase the melt rate by 10 m/year. Inclusion of Smith Glacier lowers R2 by 0.1. A quadratic fit of the type predicted for tidally-induced basal melting (*26*) would lower R2 by 0.1.